Journal Name

ARTICLE

# Molecular Composition of Organic Aerosols at Urban Background and Road Tunnel sites using Ultra-high Resolution Mass Spectrometry

Received 00th January 20xx,
Accepted 00th January 20xx

DOI: 10.1039/x0xx00000x

www.rsc.org/

Haijie Tong [a†], Ivan Kourtchev[a], Pallavi Pant[b], Ian J. Keyte[b], Ian P. O'Connor[c], John C. Wenger[c], Francis D. Pope[b], Roy M. Harrison[b††], Markus Kalberer [a]*

Organic aerosol composition in the urban atmosphere is highly complex and strongly influenced by vehicular emissions which vary according to the make-up of the vehicle fleet. Normalized test measurements do not necessarily reflect real-world emission profiles and road tunnels are therefore ideal locations to characterise realistic traffic particle emissions with minimal interference from other particle sources and from atmospheric aging processes affecting their composition. In the current study, the composition of fine particles (diameter ≤2.5 µm) at an urban background site (Elms Road Observatory Site) and a road tunnel (Queensway) in Birmingham, UK, were analysed with direct infusion, nano-electrospray ionisation ultrahigh resolution mass spectrometry (UHRMS). The overall particle composition at these two sites is compared with an industrial harbour site in Cork, Ireland, with special emphasis on oxidised mono-aromatic, polycyclic aromatic hydrocarbons (PAHs) and nitro-aromatics. Different classification criteria, such as double bond equivalents, aromaticity index and aromaticity equivalent are used and compared to assess the fraction of aromatic components in the approximately one thousand oxidized organic compounds at the different sampling locations.

## 1. Introduction

Aerosol particles are emitted into the atmosphere by natural and anthropogenic processes and about 20-90% of submicron particles are composed of organic material[1, 2]. Road traffic and especially engine exhaust emissions are responsible for a substantial fraction of urban submicron particles[3]. In addition to directly emitted particles, combustion engines can emit significant amounts of gaseous volatile organic compounds which can generate additional particle mass due to gas-to-particle conversion processes such as oxidation reactions leading to less volatile organic compounds and the formation of so-called secondary organic aerosol mass (SOA)[4, 5]. The chemical composition of road traffic related exhaust particles is highly complex and especially the effects of SOA formation and atmospheric aging, which alter the particle composition during their entire lifetime, are not well understood. The particle composition also depends on traffic characteristics such as vehicle fleet composition and the type of fuel used or meteorological conditions such as long range atmospheric transport[6, 7]. In addition to traffic there are a large number of other natural and anthropogenic sources contributing to urban particle mass. Assessment of the most important particle sources and their contribution to the ambient particle mixture is only possible through a detailed chemical characterisation of ambient particles and the major potential sources. Inhalation of these particles has been linked to a number of adverse health effects[8, 9] and carcinogenic compounds

[a] Centre for Atmospheric Science, University of Cambridge, Lensfield Road, Cambridge, CB2 1 EW, UK. E-mail: markus.kalberer@atm.ch.cam.ac.uk
[b] School of Geography, Earth and Environmental Sciences, University of Birmingham, Edgbaston, Birmingham, B15 2TT, UK.
[c] Department of Chemistry and Environmental Research Institute, University College Cork, Cork, Ireland.
† Present address: Max Planck Institute for Chemistry. Hahn-Meitner-Weg 1, 55128 Mainz, Germany
†† Also at: Department of Environmental Sciences / Center of Excellence in Environmental Studies, King Abdulaziz University, PO Box 80203, Jeddah, 21589, Saudi Arabia

such as polycyclic aromatic hydrocarbons (PAHs) and transition metals are potentially responsible for their toxicity[10-12].

Particles emitted by an average vehicle fleet at a specific location can be assessed ideally with samples collected in road tunnels because they provide a real-world mixture of vehicles and driving conditions. Currently only a few studies have focused on traffic emission in urban aerosol in the UK[13, 14]. These studies utilized a range of traffic-specific organic markers, such as hopanes, steranes and PAHs,, which allows source apportionment of different traffic sources. However, the huge complexity of combustion exhaust particles with thousands of organic compounds[15] warrants a broad characterisation of the organic particle composition to potentially complement existing particle source profiles.

In our current study direct infusion negative nano-electrospray ionisation (nanoESI) ultrahigh resolution mass spectrometry (UHR-MS) was used to characterise and compare a broad range of particle components in fine particles from a road tunnel, characteristic of directly emitted vehicle exhaust particles, and an urban background site in Birmingham, UK. The results show that in both sampling locations a large number of oxidised mono-aromatic compounds and PAHs are present with significant numbers of nitrogen-containing aromatic compounds, especially in the tunnel samples. In contrast, sulfur-containing organics have greater relative abundance at the urban background site, indicating the effect of atmospheric aging processes or the presence of non-traffic sources.

## 2. Method

### 2.1 Sample collection and analysis

Sampling was conducted at the A38 Queensway Tunnel (QT) and the Elms Road Observatory Site (EROS) in Birmingham, UK, between September 11 and 21, 2012. Five filter samples were analysed from each site (Table 1). More detailed information about the sampling sites is given elsewhere (Pant et al., submitted).

Briefly, the Queensway tunnel is naturally ventilated, 545 metres long and in North/South direction allowing 50 kilometres/hour vehicle speed. It has two lanes on each side and a 25 $m^2$ cross-section. The daily traffic volume through the tunnel is around 25000 vehicles (Pant et al., submitted). The aerosol samplers were placed in the emergency layby area at a distance of 1.5 m from the road in the southbound lane. The EROS site was chosen as an urban background site, located at 52.45° N, 1.93° W, about 3.5 km southwest of Birmingham city centre with no significant particle sources in the immediate vicinity of the site. At both sites 24 hour integrated $PM_{2.5}$ aerosol samples were collected on pre-baked 150 mm quartz filters (Whatman QM-A) using a high-volume samplers (Digitel DHA-80) operating at a flow rate of 500 L $min^{-1}$.

Organic carbon (OC) and elemental carbon (EC) concentrations of all aerosol samples were determined using a Sunset Laboratory thermal/optical carbon analyser using the EUSAAR2 protocol[16] and results are shown in Table 1.

Detailed information on the aerosol sample extraction and UHRMS analysis can be founded elsewhere[17]. Briefly, a part of the quartz fibre filter (35±7 $cm^2$) was extracted three times with 5 mL of methanol (Optima® LC/MS grade, Fisher Scientific) under ultrasonic agitation for 30 min in ice cold water. The extracts were combined, filtered through a 0.2 µm ISO-Disc™ PTFE filter (Supelco, Bellefonte, PA, USA), reduced by volume to the same OC concentration under a gentle stream of nitrogen. The extracts were analysed using an ultrahigh resolution LTQ Orbitrap Velos mass spectrometer (Thermo Fisher, Bremen, Germany) equipped with a TriVersa Nanomate robotic nanoflow chip-based electrospray ionisation (ESI) source (Advion Biosciences, Ithaca NY, USA)[18].

The Orbitrap MS was calibrated using an Ultramark 1621 solution (Sigma-Aldrich, UK) providing mass accuracy of the instrument below 1 ppm. The instrument mass resolution was 100000 at *m/z* 400. The direct infusion, negative mode nanoESI parameters were as follows: the ionization voltage and backpressure were set at -1.4 kV and 0.8 psi, respectively. The inlet temperature was 200 $^0$C.

The mass spectral data analysis was performed using procedures described in detail elsewhere [17]. Briefly, for each sample analysis, 60–90 mass spectral scans were averaged into one mass spectrum. The high mass resolution and accuracy measurements allows for an unambiguous assignment of formulas for most peaks in the mass spectra up to a mass range of about m/z 450[19]. Molecular assignments were made using Xcalibur 2.1 software (Thermo Fisher Scientific, USA) applying the following constraints $0<{}^{12}C\leq100$, $^{13}C\leq1$, $^{1}H\leq200$, $^{16}O\leq50$, $^{14}N\leq5$, $^{32}S\leq2$, $^{34}S\leq1$. The double bond equivalent (DBE) for each individual formula was calculated using Xcalibur 2.1 software. All molar ratios, DBE factors and chemical formulae presented in this paper refer to neutral molecules. Data processing was performed using a Mathematica

 

10.1 (Wolfram Research Inc., UK) code developed in-house that employed several conservative rules and constraints to identify unambiguous elemental formulas for measured accurate mass spectral peaks as discussed in more detail in our previous studies[17, 20]. Briefly, the assigned formulas were checked to satisfy the nitrogen-rule. Elemental formulae containing $^{13}C$ or $^{34}S$ were checked for the presence of $^{12}C$ or $^{32}S$ counterparts respectively, and if they were not present the formula with the next larger mass error was considered. The background spectra obtained from the procedural blanks were also processed using the rules mentioned above. The formulae lists of the background spectra were subtracted from those of the ambient samples and only formulae with a sample to background ratio $\geq$10 were retained[17,20].

The samples from the two Birmingham site are compared to aerosol collected at an industrial harbour site in Cork, Ireland. The sampling and analysis of these samples are described elsewhere in detail[18].

### 2.2 Interpretation of direct-injection electrospray ionisation high-resolution mass spectrometry data

Only ions found in all five tunnel or all five background samples, respectively, referred to as 'common ions' in the text, were considered in the analysis presented here. These common ions represent the compounds present in the aerosol at a specific site over several days, which ensures they represent a typical average traffic source profile and an average urban organic background profile, respectively.

Electrospray ionisation UHRMS is a highly sensitive mass spectrometry technique to analyse polar compounds and due to its soft ionisation process analyte fragmentation is minimal, which allows characterisation of complex samples without prior chromatographic separation[21, 22,23]. However, non-polar compounds (such as alkanes or non-oxidised aromatic compounds) cannot be ionised and measured with ESI or only with very poor ionisation efficiencies[24]. In addition, all ESI techniques are prone to matrix effects, which cause varying ionisation efficiency (and therefore signal intensities) depending on the overall sample composition (i.e. matrix). By considering common ions only we minimize sample-to-sample variations due to these matrix effects and obtain mass spectra representative for the respective sampling locations.

This study aims to compare and contrast differences in the chemical composition of the about 1000 common ion formulae measured at the three urban sites. This reflects the chemical diversity and complexity of particles at the various sampling sites but does not allow for inferring concentrations of compounds due to the ionisation efficiency effects discussed above (matrix effects).

## 3. Results and discussion

A main emphasis of this study is to characterise the very broad and complex composition of oxidized organic compounds (formulae) in the Birmingham tunnel samples and compared them with the aerosol composition at the Birmingham urban background and the Cork harbour sites with the goal to identify compositional influences of traffic exhaust emissions (i.e. the tunnel samples) on ambient urban particle composition.

The mass spectra in Figure 1a and 1b show common ions of the five samples collected at the background and the tunnel site. As described above, the common ions represent those mass spectral peaks that are present over several days at the locations and can thus be seen as robust profile for the average traffic source at the Queensway tunnel in Birmingham (Figure 1b) and average Birmingham urban background composition (Figure 1a). In total about 970 and 1000 common ions were detected in the background and tunnel samples, respectively.

Figure 1 clearly shows that formulae containing only C, H and O atoms (i.e. containing no nitrogen and sulfur functional groups, red peaks in Figure 1) are the dominant formula subgroup in both the urban background and the tunnel particles with a fraction of ~ 40% and ~ 44% (384 and 439 ions) respectively. This compares to an earlier study where we observed about 60% of all ions in the CHO-subgroup at an industrial harbour site in Cork, Ireland.

N-containing formulae (CHON subgroup) make up about 28% of the background sample and 39% of the tunnel sample (see more detailed discussion below). In contrast, S-containing organics (i.e. CHOS and CHONS subgroups) were more prominent in the urban background samples compared to the tunnel samples. This is likely reflecting the longer atmospheric aging and heterogeneous

reactions of particle components collected at the background site with sulphate and sulfuric acid present in greater abundance in urban background particles compared to particles at the tunnel site which represent more direct emission conditions with low sulfur content[25, 26].

There is significant overlap between the number of molecular formulae (including N and S-containing organics) at both the Birmingham tunnel and the background site (~60%), as shown in the Venn diagram (Figure 1c), indicating that the chemical composition of particles at the background site might be significantly impacted by traffic emissions. It must be noted, however, that the online ESI-MS technique used in this study is only semi-quantitative as discussed above and therefore additional (e.g. chromatography) analyses would be needed to confirm these similarities on a quantitative level.

Figure 2 shows van Krevelen plots for the common ions of the Birmingham background, the tunnel and the Cork samples where H/C (hydrogen to carbon) versus O/C (oxygen to carbon) elemental ratios of all formulae detected in these samples indicate the degree of oxidation[17, 18, 27, 28]. The color code in Figure 2 indicates the double bound equivalent (DBE) value of each formula. The DBE is calculated as[29]

$$\mathrm{DBE} = 1 - \frac{\mathrm{N_H}}{2} + \frac{\mathrm{N_N}}{2} + \frac{\mathrm{N_S}}{2} + \mathrm{N_C} \quad (1)$$

Where 'N' is the number of atoms (C, H, N, and S) in a formula of $C_cH_hO_oN_nS_s$.

The less oxidised and hydrogen-rich formulae (H/C>1.5) at all three locations are likely aliphatic compounds. Previous studies that utilised UHRMS attributed some of these molecules to fatty acids[17, 30]. Fatty acids are a signature of a number of primary natural sources, including marine biota[31], plant waxes[32], and combustion of biomass material[33, 34]. Although less abundant than in the background site, a significant number of these aliphatic compounds are also found in the tunnel sample suggesting that vehicle emissions are also a potential source of these saturated aliphatic compounds.

Formulae with 0<H/C≤1.0 and O/C≤0.5 (dotted-line squares in Figures 2a, 2b, 2c) dominantly have high DBE values (≥7.0), which is consistent with oxidized polycyclic aromatic hydrocarbons (PAHs; the smallest PAH, naphthalene, $C_{10}H_8$ has an H/C of 0.8 and 7 DBE). The highest number of these PAH-like compounds is found in the tunnel samples with 480 ions (48% of all peaks in the tunnel samples), compared to only 186 ions in the urban background samples (19%). The samples from Cork harbour contains 110 ions in the PAH range (38%). The comparable fraction of high-DBE formulae in the tunnel and Cork harbour samples likely reflects the traffic and industrial activity influencing particle composition at these sites.

To evaluate further whether this large number of formulae with high DBEs are indeed of oxidized (poly-)aromatic structure the formulae in the CHO subgroup were probed in more detail. Figure 3a-3c shows the H/C ratio of all CHO subgroup formulae as a function of their molecular weight and Figure 3d-3f the O/C ratio at all three locations. Figure 3a (Birmingham urban background) and 3b (Birmingham tunnel) show that H/C of most of the formulae are larger than 1.0. Only a small fraction of the formulae (~ 21% for background and ~ 36% for tunnel) have H/C<1.0. Figure 3 clearly shows that most formulae with a DBE > 10 have molecular masses > 200 Da, which is consistent with slightly oxidized 3-ring PAHs (e.g., dihydroxy-anthracenes) and larger polyaromatics. A similar profile of high-mass, high-DBE formulae is present in the Cork harbour samples (Figure 3c, 3f).

The vast majority of the high-DBE (PAH-like) compounds have low or moderate O/C ratios with values mostly between 0.2 – 0.5. This is rather low compared to many other, often highly oxidized organic compounds in ambient aerosols[18, 35]. For PAHs, however, these O/C ratios represent a high degree of oxidation: using again the example of anthracene ($C_{14}H_{10}$), an O/C ratio of about 0.3 would correspond to 4-5 oxygen atoms in the molecule.

DBE and molecular mass can however be inadequate to identify whether a specific molecular formula is potentially a (poly-) aromatic structure. Therefore, two parameters were developed in recent years, the Aromaticity Index (AI) and Aromaticity Equivalent ($X_c$) to characterize aromatic and poly-aromatic compounds in highly complex compound mixtures[36, 37]. The AI is a measure of the C-C double bond density by considering the contribution of heteroatoms to π–bonds, which normally has a range of 0 to 1. The AI can be calculated for each formula determined in a UHRMS spectrum and is calculated as[36]

 

$$\mathrm{AI} = \frac{\mathrm{DBE_{AI}}}{\mathrm{C_{AI}}} = \frac{1+\mathrm{N}_C-\mathrm{N}_O-\mathrm{N}_S-0.5\mathrm{N}_H}{\mathrm{N}_C-\mathrm{N}_O-\mathrm{N}_S-\mathrm{N}_N} \quad (2)$$

Where the 'N' in equations (2) to (5) is the atom number for H, C, O, N, or S. $DBE_{AI}$ is the minimum number of C-C double bonds plus rings in the molecule. The $DBE_{AI}$ and $C_{AI}$ were calculated through following equations:

$$\mathrm{DBE_{AI}} = 1 + \mathrm{N}_C - \mathrm{N}_O - \mathrm{N}_S - 0.5\mathrm{N}_H \quad (3)$$

$$\mathrm{C_{AI}} = \mathrm{N}_C - \mathrm{N}_O - \mathrm{N}_N - \mathrm{N}_S \quad (4)$$

The AI value of > 0.5 is indicative of aromatic compounds and AI ≥ 0.67 of PAHs. However, for (poly-)aromatic compounds with significant alkylation AI values drop below these thresholds and can thus be wrongly assigned as non-aromatic structures. To avoid such mis-classifications an improved "Aromaticity Equivalent" parameter $X_c$ has been proposed[37]. $X_c$ normally has values between 0 and 3.0 and is calculated by the following equation[37]:

$$\mathrm{X}_c = \frac{3(\mathrm{DBE}-\mathrm{mN}_O-n\mathrm{N}_S)-2}{\mathrm{DBE}-\mathrm{mN}_O-\mathrm{nN}_S} \quad (5)$$

Where the parameters of 'm' and 'n' in equation (5) account for the fraction of oxygen and sulfur atoms involved in π–bond structures of a compound and are different for different functional groups. For carboxylic acid, ester, and nitro functional groups m=n=0.5[37]. For compounds with other functional groups such as aldehydes, ketones, nitroso, cyanate, alcohol, or ethers 'm' and 'n' need to be adjusted to 1 or 0. Because electrospray ionisation, used in this study, is most sensitive to carboxylic acids the $X_c$ analysis below was performed assuming m=n=0.5. When the molecular formula had an odd number of oxygen or sulfur, the sum ($mN_O$+$nN_S$) in equation (5) was rounded down to the closest integer as detailed elsewhere [37].

The DBE values versus the number of carbon atoms as well as AI values for all CHO subgroup formulae in the Birmingham background and tunnel samples are shown in Figure 4a. The peak intensity is indicated by the size of symbols and naphthalene ($C_{10}H_8$) and anthracene ($C_{14}H_{12}$) are shown as red crosses in Figure 4a and 4b. The vast majority of compounds at the background site (circles) have very low DBE (< 5) and AI (≤ 0.5, grey symbols) values demonstrating the low abundance of oxidised mono-aromatics and PAHs at this site. There is only a limited number of formulae with AI values of 0.53 - 0.67 (32 formulae) and ≥ 0.67 (6 formulae) in the background sample, which are the thresholds for mono-aromatics and polyaromatics, respectively. This is in contrast to the tunnel samples (Figure 4a, triangles) where a larger number of formulae have AI values of 0.53 - 0.67 (65 formulae; mono-aromatics) and AI ≥ 0.67 (22 formulae) indicating the presence of more oxidised PAHs than at the background site.

Figure 4b shows the same data as Figure 4a but the color code indicates the value of $X_c$. Using the $X_c$ classification there are 128 formulae in the background samples with an $X_c$ value between 2.5 and 2.71 (indicative of mono-aromatics), significantly more than the AI classification suggests. Similarly, $X_c$ suggests that more PAHs are present in the background sample than the AI classification with 44 formulae having $X_c$ > 2.71. The tunnel samples also contain a larger number of formulae consistent with mono-aromatic (173 formulae, blue and brown triangles, Figure 4b) and poly-aromatic structure (106 formulae, pink and purple triangles, Figure 4b).

The considerably larger number of PAHs identified using the $X_c$ classification compared to the AI suggests that there is a large number of alkylated PAHs, which are wrongly assigned as non-aromatic by the AI classification.

Figure 4a and 4b highlight the advantage of the AI and especially of the $X_c$ classification compared to using only DBEs as indicator of aromaticity or PAHs. When only considering DBEs, all formulae with a DBE ≥ 7 have to be assumed to be potentially PAHs. However, Figure 4 shows that there are a significant number of formulae with 7 or more DBEs (76 formulae for the background and 101 formulae for tunnel samples), which cannot be explained by polyaromatic structures using the more detailed concepts of AI or $X_c$ (blue and green data points in Figure 4 with DBE >7).

Overall there are more mono-aromatics at the Birmingham background and tunnel site (using $X_c$) with 128 and 173 formulae, respectively, than PAHs (44 formulae at background and 106 at tunnel site). The much lower number of oxidised (poly-)aromatics at the background site is likely due to dilution affecting the background site more that the tunnel samples. Importantly, 41 of the PAHs detected in the tunnel samples were also present at the background site (out of 44 PAHs detected in the background sample) suggesting that almost all PAHs detected at the background site have a contribution from traffic exhaust sources.

Figure 5 shows the H/C (a, b, and c) and O/C ratios (d, e, and f) versus the neutral mass and $X_c$ of the Birmingham background (a and d), Birmingham tunnel (b and e), and Cork harbour (c and f) samples. This illustrates clearly the much larger number of mono-aromatic compounds (blue and green data points) compared to PAHs (pink to purple). The mass range and O/C ratio of mono-aromatics shows the presence of a high degree of oxidation (O/C up to ca. 0.7) and alkylation (molecular masses up to about 330 Da). In contrast, oxidised PAHs are less abundant and their lower H/C ratio (compared to mono-aromatics) with values of mostly below 1 indicates a generally low degree of alkylation. The industrial harbour site in Cork has a more balanced fraction of mono-aromatics and PAHs.

The O/C ratios of organic compounds can be misleading when assessing the degree of oxidation because non-oxidative reactions (such as dehydrogenation) can change the O/C but may not affect the degree of oxidation of a compound. Thus, an alternative metric, the 'carbon oxidation state', has been applied to characterizer aerosols composition[38] and can be calculated through the following equation:

$$\overline{OS}_C = -\sum_i OS_i \frac{N_i}{N_C} \quad (6)$$

Where the $\overline{OS}_C$ is the average carbon oxidation state. $OS_i$ is the oxidation state associated with element I, $N_i$ and $N_C$ are moles of elements *i* and of carbon, respectively. For the application of $\overline{OS}_C$ to CHO subgroup formulae only, equation (6) can be simplified to:

$$\overline{OS}_C \approx 2\,{}^{O}\!/_{C} - {}^{H}\!/_{C} \quad (7)$$

Where O/C and H/C are the elemental ratio of oxygen and hydrogen to carbon, respectively. The carbon oxidation states of all CHO subgroup formulae in the Birmingham background and tunnel samples are shown in Figure 6, with their corresponding $X_c$ as color code. Especially in the tunnel samples aromatics and poly-aromatics are generally at the higher end of the distributions of $\overline{OS}_C$ values for a particular carbon number and almost all PAHs ($X_c$ > 2.7) have a $\overline{OS}_C$ > -0.6. Such high $\overline{OS}_C$ are generally associated with semi- or low-volatility aerosol components.

In general, upper limit $\overline{OS}_C$ values are 1 for both Birmingham samples, which is lower compared to pure secondary organic aerosol (from chamber studies) where $\overline{OS}_C$ goes up to 2, demonstrating the relatively fresh nature of most components in these urban particles and compared to remote locations where long-range transport and oxidation cause a higher degree of oxidation[30].

Besides CHO-containing compounds there are a considerable number of organic compounds containing nitrogen and sulfur (Figure 1). Figure 7 shows three different subgroups, (CHON, CHOS, and CHONS), while CHN, CHS, and CHNS components are not included because they account for < 0.5% of the total formulae in the samples. At the Birmingham background site (Figure 7a) the CHON subgroup is the dominant compound group with about 47 % of all N- or S-containing formulae. Only a relatively small number of components (81 CHON formulae, 7 CHOS formulae, 5 CHONS formulae) have $X_c \geq 2.5$ (at the background samples) and thus can be categorized as N- or S-containing aromatic compounds. The tunnel samples (Figure 7b) have much larger number fraction of CHON components (391 formulae, ~ 70%) indicating a higher degree of nitration. The higher number of aromatic structures (303 CHON formulae with $X_c \geq 2.5$) in the tunnel samples supports the presence of many nitro-(poly-)aromatics.

A comparison of Figure 3 (panels a, b, d and e) and Figure 7 shows that aromatic compounds in the Birmingham tunnel samples with DBE≤9, H/C<1, O/C<0.7, and neutral mass <300 contain a significant fraction of CHON subgroup formulae. In contrast, the aromatic compounds in the urban background samples in the same DBE, H/C, and O/C value range are mainly composed of CHO subgroup formulae and only contain a small fraction of CHON, CHOS, or CHONS components.

The most intensive N-containing compound in the mass spectra from tunnel samples was an ion at *m/z* 138.01988 (RI> 65%) with a molecular formula $C_6H_5NO_3$, possibly corresponding to nitrophenols (2-nitrophenol and/or 4-nitrophenol). Formulae with likely the same core-structure but with additional one and two methyl groups (i.e. $C_7H_7NO_3$ and $C_8H_9NO_3$) were also detected. These compounds have been previously observed in aerosol from

 

urban locations e.g., Rome, Italy[39], Mainz, Germany[40] and Cork, Ireland[18] and were mainly attributed to traffic emissions. However, nitrophenols were previously also found in various other sources including decomposition of herbicides and insecticides and burning of coal and wood[41], although in urban environments primary vehicle engine emissions are believed to be their major source[42]. Another nitrogen-containing homologous series observed with high signal intensities included molecules with the following molecular formulae $C_6H_5NO_4$, $C_7H_7NO_4$, $C_8H_9NO_4$, $C_9H_{11}NO_4$ and $C_{10}H_{13}NO_4$. These formulae were tentatively identified as nitroaromatic compounds, e.g., nitrocatechols, nitrophenols, nitroguaiacols and nitrosalicylic acids. These nitroaromatics have been recently detected in aerosol samples from urban locations, e.g., Ljubljana, Slovenia[43] and rural environments e.g., Saxony, Germany[44], K-Puszta, Hungary[45], Hyytiälä, Finland[17], Los Angeles, USA[46] and Cork, Ireland[18] and were mainly attributed to biomass burning sources. Although direct infusion analysis does not allow structural or isomeric molecular elucidation, our results suggests that these identified series can be associated not only with biomass burning but also with traffic emission sources. In addition, formulae with OSc < −1 and more than 7 carbon atoms, which is indicative of primary biomass burning aerosol[38], were observed in the background Birmingham samples (Fig 6). Their small fraction compared to the overall observed number of formulae (ca. 8%) suggest a rather modest influence of biomass burning at the Birmingham background site compared to traffic sources.

Only a very small number of known oxidized and nitrated PAHs were detected in the Birmingham background and tunnel samples, e.g. formulae that correspond to nitro-naphthalenes and hydroxy-nitro-naphthalenes. These formulae were measured with low signal intensities, which is likely due to their poor ionisation efficiency in negative mode ESI-MS.

Using gas chromatography – mass spectrometry samples from the same two locations in Birmingham were analysed and several nitro-PAHs and oxidized PAHs with a carbonyl functional groups were identified[47]. These detailed chromatography analyses concluded that PAHs at the background cite were dominated by traffic emissions, which is supported by the analyses presented here, but that other sources such as wood burning became increasingly important over the last two decades. This study[47] also provided strong evidence of increased levels of nitro-PAHs in the tunnel samples, likely due to increased use of diesel cars, which is also supported by the nitro-aromatics identified in the current study.

Formulae in the CHOS subgroup are more prominent in the background sample (~ 36% of all N or S containing formulae) than in the tunnel samples (~ 24%). The higher number of CHOS components at the background site could be explained by atmospheric aging reactions of organics with $H_2SO_4$ leading to the formation of organosulfates. The number of aromatic sulphates (using AI or $X_c$), however, is very small in both samples (less than 10 formulae).

The composition of the tunnel samples shows a distinct boundary between CHON and S-containing subgroups (CHOS and CHONS) (dotted line in Figure 7 b). Above this line, CHOS and CHONS subgroups are dominating whereas below the line, CHON subgroup formulae are most abundant. Thus CHOS and CHONS components have on average a larger H/C ratio than the CHON compounds. About 91% of the 168 CHOS and CHONS compounds have ≥ 4 oxygen atoms and are likely organosulfates. This clear distinction in the H/C ratio between S- and N-containing compounds is not observed in the Birmingham background samples where on average the CHON subgroup has a higher H/C ratio than in the tunnel samples.

As shown in Figure 8a about 96% of all molecular formulae associated with mono-aromatic compounds found in background Birmingham samples were also present in tunnel samples. A slightly smaller but still very high fraction of PAH-like molecular formulae (~87%) from the background samples were also present in the tunnel aerosol indicating that the majority of these molecules at the background site are likely to be associated with the traffic emissions.

## 4. Conclusions

The organic composition of ambient aerosol was analysed and compared from a road tunnel, an urban background and industrial harbour sites using direct infusion, negative mode nanoESI UHR-MS. Components of the CHO-subgroup (containing only C, H and O atoms) were most dominant at all sites. A higher number of mono-aromatics and PAHs were identified in the tunnel samples compared to the urban

background sites. Double bond equivalents, aromaticity index and aromaticity equivalent approaches were compared to identify the distribution of oxidized mono-aromatics and PAHs among the about one thousand organic compounds (formulae) present in the mass spectra at these sites.

Nitrogen- and sulfur-containing formulae were also investigated and a higher number of N-containing mono-aromatics were observed in the tunnel samples compared to the background samples with some nitro-aromatic compounds tentatively identified. In contrast, a higher fraction of S-containing formulae, likely organic-sulphates, were found in the urban background site, indicating the influence of atmospheric aging processes or the presence of non-traffic sources.

Using common ions from the tunnel samples integrated over five days represents a robust average organic composition profile of vehicle emissions and our results suggest that traffic emission can be a source for a very large number of oxidised mono-aromatics and PAHs in the urban atmosphere, which could potentially be used to better characterise and constrain vehicle exhaust emission profiles and effects of atmospheric aging on these particle emission.

Although direct-injection ESI-UHRMS analyses (performed in this study) allow separating 1000s of compounds in a single analysis they cannot unambiguously identify individual compounds at a molecular level. In addition, ESI-MS is mostly sensitive to compounds with polar functional groups. Thus, combining ESI-UHRMS data with results from other techniques, which are sensitive to less polar organic compounds and are capable of separating 1000s of compounds in a single analysis such as two-dimensional gas chromatography - mass spectrometry might be a promising approach to characterize comprehensively the entire organic compositional complexity in atmospheric particles on a molecular level.

## Acknowledgements

We would like to thank Olalekan Popoola at University of Cambridge for helping to improve the Mathematica code for mass spectral data evaluation. We thank Salim Azzi, John Poole, Paul Lees and Amey plc in general for access to the Queensway Tunnel. PP acknowledges financial support from the University of Birmingham. Financial support by ERC grant 279405 is acknowledged.

## Notes and references

1. J. Jimenez, M. Canagaratna, N. Donahue, A. Prevot, Q. Zhang, J. Kroll, P. DeCarlo, J. Allan, H. Coe and N. Ng, *Science*, 2009, **326**, 1525-1529.
2. M. Kanakidou, J. Seinfeld, S. Pandis, I. Barnes, F. Dentener, M. Facchini, R. V. Dingenen, B. Ervens, A. Nenes and C. Nielsen, *Atmos. Chem. Phys.*, 2005, **5**, 1053-1123.
3. A. Q. E. GROUP, *Fine Particulate Matter (PM2.5) in the United Kingdom*, Department for Environment, Food and Rural Affairs, London., 2012.
4. S. Platt, I. E. Haddad, S. Pieber, R.-J. Huang, A. Zardini, M. Clairotte, R. Suarez-Bertoa, P. Barmet, L. Pfaffenberger and R. Wolf, *Nat. Commun.*, 2014, **5**, 3749.
5. D. R. Gentner, G. Isaacman, D. R. Worton, A. W. Chan, T. R. Dallmann, L. Davis, S. Liu, D. A. Day, L. M. Russell and K. R. Wilson, *Proc. Natl. Acad. Sci. U. S. A.*, 2012, **109**, 18318-18323.
6. P. Pant and R. M. Harrison, *Atmos. Environ.*, 2013, **77**, 78-97.
7. V. Franco, M. Kousoulidou, M. Muntean, L. Ntziachristos, S. Hausberger and P. Dilara, *Atmos. Environ.*, 2013, **70**, 84-97.
8. D. Brugge, J. L. Durant and C. Rioux, *Environ. Health*, 2007, **6**, 23.
9. N. Künzli, R. Kaiser, S. Medina, M. Studnicka, O. Chanel, P. Filliger, M. Herry, F. Horak, V. Puybonnieux-Texier and P. Quénel, *Lancet*, 2000, **356**, 795-801.
10. U. Pöschl and M. Shiraiwa, *Chem. Rev.*, 2015, **115**, 4440-4475.
11. I. J. Keyte, R. M. Harrison and G. Lammel, *Chem. Soc. Rev.*, 2013, **42**, 9333-9391.
12. K. Slezakova, D. Castro, C. Delerue–Matos, M. da Conceição Alvim–Ferraz, S. Morais and M. do Carmo Pereira, *Atmos. Res.*, 2013, **127**, 141-147.
13. R. M. Harrison, R. Tilling, M. a. S. C. Romero, S. Harrad and K. Jarvis, *Atmos. Environ.*, 2003, **37**, 2391-2402.

 

14. D. Smith and R. M. Harrison, *Atmos. Environ.*, 1996, **30**, 2513-2525.
15. C. P. Rüger, T. Miersch, T. Schwemer, M. Sklorz and R. Zimmermann, *Anal. Chem.*, 2015.
16. F. Cavalli, M. Viana, K. Yttri, J. Genberg and J.-P. Putaud, *Atmos. Meas. Tech.*, 2010, **3**, 79-89.
17. I. Kourtchev, S. Fuller, J. Aalto, T. M. Ruuskanen, M. W. McLeod, W. Maenhaut, R. Jones, M. Kulmala and M. Kalberer, *Environ. Sci. Technol.*, 2013, **47**, 4069-4079.
18. I. Kourtchev, I. O'Connor, C. Giorio, S. Fuller, K. Kristensen, W. Maenhaut, J. Wenger, J. Sodeau, M. Glasius and M. Kalberer, *Atmos. Environ.*, 2014, **89**, 525-532.
19. N. W. Green and E. M. Perdue, *Anal. Chem*, 2015, **87**, 5086-5094.
20. I. Kourtchev, J.-F. Doussin, C. Giorio, B. Mahon, E. Wilson, N. Maurin, E. Pangui, D. Venables, J. Wenger and M. Kalberer, *Atmos. Chem. Phys.*, 2015, **15**, 5683-5695.
21. C. M. Whitehouse, R. N. Dreyer, M. Yamashita and J. B. Fenn, *Anal. Chem.*, 1985, **57**, 675-679.
22. M. Kandiah and P. L. Urban, *Chem. Soc. Rev.*, 2013, **42**, 5299-5322.
23. S. Banerjee and S. Mazumdar, *Int. J. Anal. Chem.*, 2012, **2012**, 282574.
24. L. Molnárné Guricza and W. Schrader, *J. Mass Spectrom.*, 2015, **50**, 549-557.
25. J. D. Surratt, J. H. Kroll, T. E. Kleindienst, E. O. Edney, M. Claeys, A. Sorooshian, N. L. Ng, J. H. Offenberg, M. Lewandowski and M. Jaoui, *Environ. Sci. Technol.*, 2007, **41**, 517-527.
26. P. Schmitt-Kopplin, A. Gelencser, E. Dabek-Zlotorzynska, G. Kiss, N. Hertkorn, M. Harir, Y. Hong and I. Gebefügi, *Anal. Chem.*, 2010, **82**, 8017-8026.
27. S. A. Nizkorodov, J. Laskin and A. Laskin, *Phys. Chem. Chem. Phys.*, 2011, **13**, 3612-3629.
28. Y.-H. Lin, Z. Zhang, K. S. Docherty, H. Zhang, S. H. Budisulistiorini, C. L. Rubitschun, S. L. Shaw, E. M. Knipping, E. S. Edgerton and T. E. Kleindienst, *Environ. Sci. Technol.*, 2012, **46**, 250-258.
29. F. W. McLafferty and F. Tureček, *Interpretation of mass spectra*, University Science Books, 1993.
30. I. Kourtchev, S. Fuller, C. Giorio, R. Healy, E. Wilson, I. O'Connor, J. Wenger, M. McLeod, J. Aalto and T. Ruuskanen, *Atmos. Chem. Phys.*, 2014, **14**, 2155-2167.
31. H. Tervahattu, J. Juhanoja and K. Kupiainen, *J. Geophys. Res.*, 2002, **107**, ACH 18-11-ACH 18-17.
32. B. R. Simoneit, R. Cox and L. Standley, *Atmos. Environ.*, 1988, **22**, 983-1004.
33. D. R. Oros and B. R. Simoneit, *Appl. Geochem.*, 2001, **16**, 1545-1565.
34. D. R. Oros and B. R. Simoneit, *Appl. Geochem.*, 2001, **16**, 1513-1544.
35. M. Ehn, J. A. Thornton, E. Kleist, M. Sipilä, H. Junninen, I. Pullinen, M. Springer, F. Rubach, R. Tillmann and B. Lee, *Nature*, 2014, **506**, 476-479.
36. B. Koch and T. Dittmar, *Rapid Commun. Mass Spectrom.*, 2006, **20**, 926-932.
37. M. M. Yassine, M. Harir, E. Dabek‐Zlotorzynska and P. Schmitt‐Kopplin, *Rapid Commun. Mass Spectrom.*, 2014, **28**, 2445-2454.
38. J. H. Kroll, N. M. Donahue, J. L. Jimenez, S. H. Kessler, M. R. Canagaratna, K. R. Wilson, K. E. Altieri, L. R. Mazzoleni, A. S. Wozniak and H. Bluhm, *Nat. Chem.*, 2011, **3**, 133-139.
39. A. Cecinato, V. Di Palo, D. Pomata, M. C. T. Scianò and M. Possanzini, *Chemosphere*, 2005, **59**, 679-683.
40. Y. Zhang, L. Müller, R. Winterhalter, G. Moortgat, T. Hoffmann and U. Pöschl, *Atmos. Chem. Phys.*, 2010, **10**, 7859-7873.
41. W. E. Shafer and J. Schönherr, *Ecotoxicol. Environ. Saf.*, 1985, **10**, 239-252.
42. J. Tremp, P. Mattrel, S. Fingler and W. Giger, *Water Air Soil Pollut.*, 1993, **68**, 113-123.
43. Z. Kitanovski, I. Grgić, F. Yasmeen, M. Claeys and A. Čusak, *Rapid Commun. Mass Spectrom.*, 2012, **26**, 793-804.
44. Y. Iinuma, O. Böge, R. Gräfe and H. Herrmann, *Environ. Sci. Technol.*, 2010, **44**, 8453-8459.
45. M. Claeys, R. Vermeylen, F. Yasmeen, Y. Gómez-González, X. Chi, W. Maenhaut, T. Mészáros and I. Salma, *Environ. Chem.*, 2012, **9**, 273-284.
46. X. Zhang, Y.-H. Lin, J. D. Surratt and R. J. Weber, *Environ. Sci. Technol.*, 2013, **47**, 3685-3693.
47. I. J. Keyte, University of Birmingham, 2015.

Journal Name

ARTICLE

**Table 1.** Concentration (μg $m^{-3}$) of organic carbon (OC), elemental carbon (EC), and total carbon (TC) concentrations of samples from the Birmingham background and tunnel site.

| Sample Type | Sampling Date | OC | EC | TC |
|---|---|---|---|---|
| **Tunnel** | 11.09-12.09 | 13.4 ± 0.69 | 15.1 ± 0.78 | 28.6 ± 1.47 |
| **Tunnel** | 12.09-13.09 | 19.5 ± 1.00 | 17.1 ± 0.87 | 36.6 ± 1.87 |
| **Tunnel** | 13.09-14.09 | 17.3 ± 0.89 | 18 ± 0.92 | 35.3 ± 1.81 |
| **Tunnel** | 14.09-15.09 | 20.0 ± 1.02 | 22 ± 1.12 | 42 ± 2.14 |
| **Tunnel** | 15.09-16.09 | 16.9 ±0.86 | 19.3 ± 0.99 | 36.1 ± 1.85 |
| **Background** | 11.09-12.09 | 0.41 ± 0.04 | 0.4 ± 0.04 | 0.80 ± 0.08 |
| **Background** | 12.09-13.09 | 3.12 ± 0.18 | 1.89 ± 0.12 | 5.01 ± 0.29 |
| **Background** | 13.09-14.09 | 1.25 ± 0.08 | 0.96 ± 0.07 | 2.21 ± 0.15 |
| **Background** | 14.09-15.09 | 1.42 ± 0.09 | 0.85 ± 0.06 | 2.27 ± 0.16 |
| **Background** | 15.09-16.09 | 2.05 ± 0.12 | 0.97 ± 0.07 | 3.02 ± 0.19 |

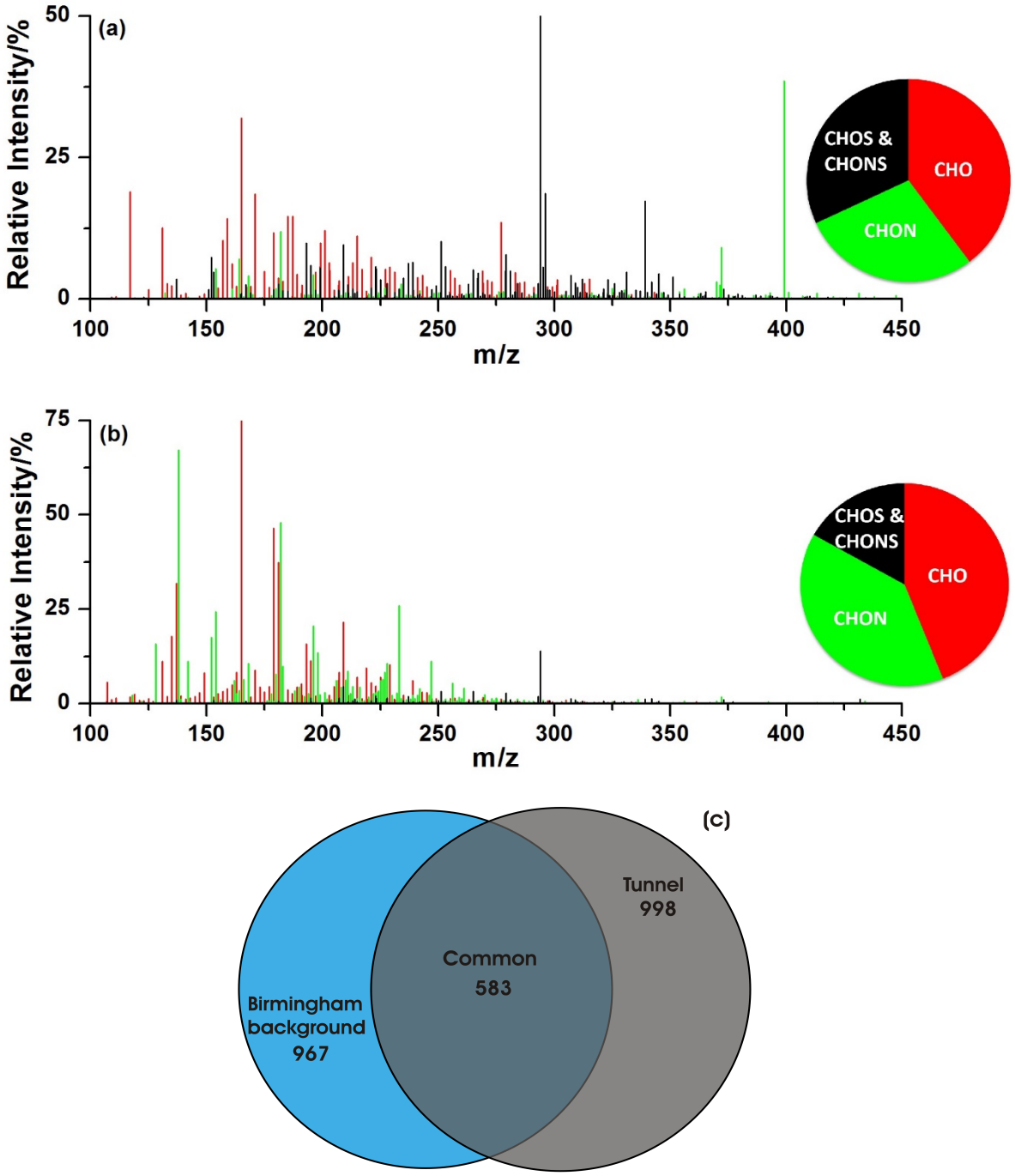


**Figure 1.** Negative ionization nanoESI mass spectra of common ions in aerosol samples collected at a background (a) and tunnel (b) site in Birmingham, UK. The pie charts and color code of the mass spectra indicate the abundance of organic compounds, which contain only C, H and O atoms and N- and S-containing compounds, respectively. Common ions are defined as ions, which are detected in all five background or five tunnel samples analysed in this study, respectively. Thus, the common ion mass spectra represent a robust signature of the organic aerosol composition at these two sites. (c) Venn diagram showing the number of all molecular formulae identified in the Birmingham tunnel and background samples and common formulae at both sites.

Journal Name

ARTICLE

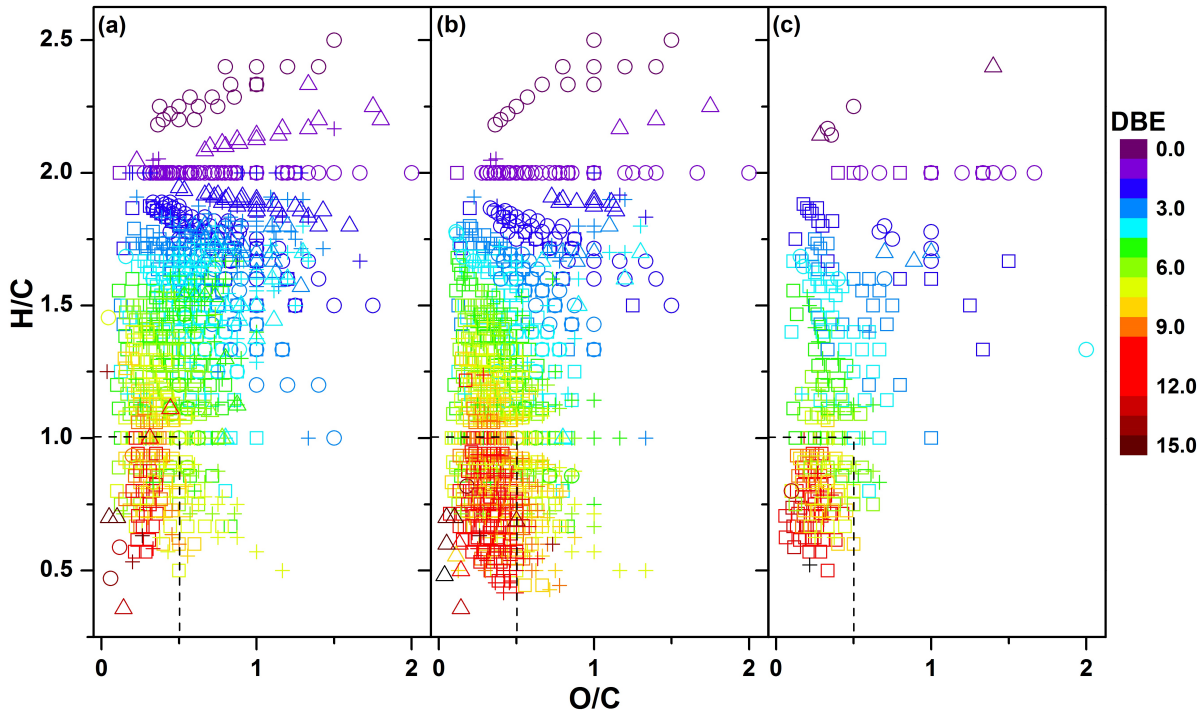


**Figure 2.** Van Krevelen diagrams (HC versus O/C atomic ratios) including double bond equivalent (DBE) values of all common ions detected in the background (a) and tunnel (b) samples from Birmingham and from Cork harbour (c). Symbols: squares indicate CHO, crosses CHON, circles CHOS, and triangles CHONS formulae. The black dashed squares indicate compounds with low H/C ratio and high DBE values, a typical signature of mono-aromatic compounds and PAHs.

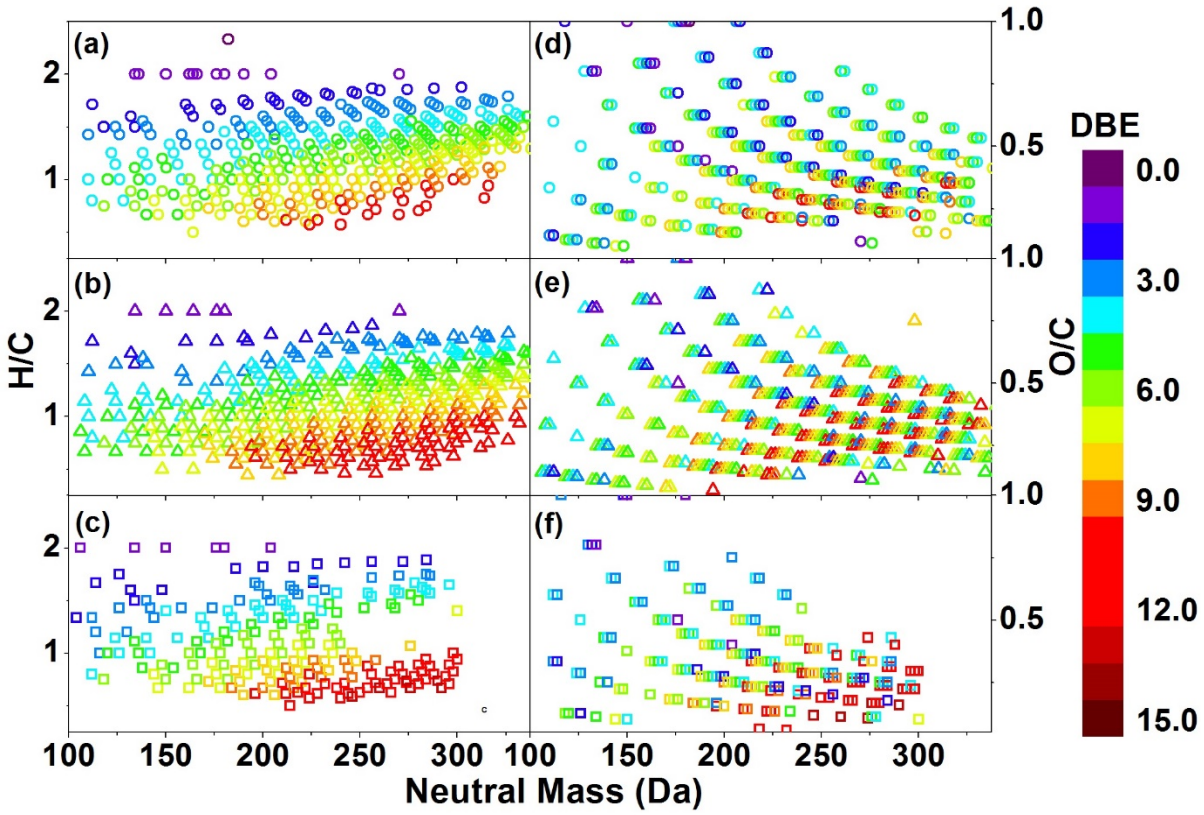


**Figure 3.** H/C (a, b and c) and O/C (d, e and f) values as a function of neutral mass and DBE values of all CHO formulae from Birmingham background (a and d), tunnel (b and e) and Cork harbour (c and f) samples. The fractions of compounds with O/C >1.0 for all samples is < 2% and these are not shown. The high number of formulae with DBE>7, masses >200Da and H/C<1 supports the presence of a large number of oxidized PAHs.

Journal Name

ARTICLE

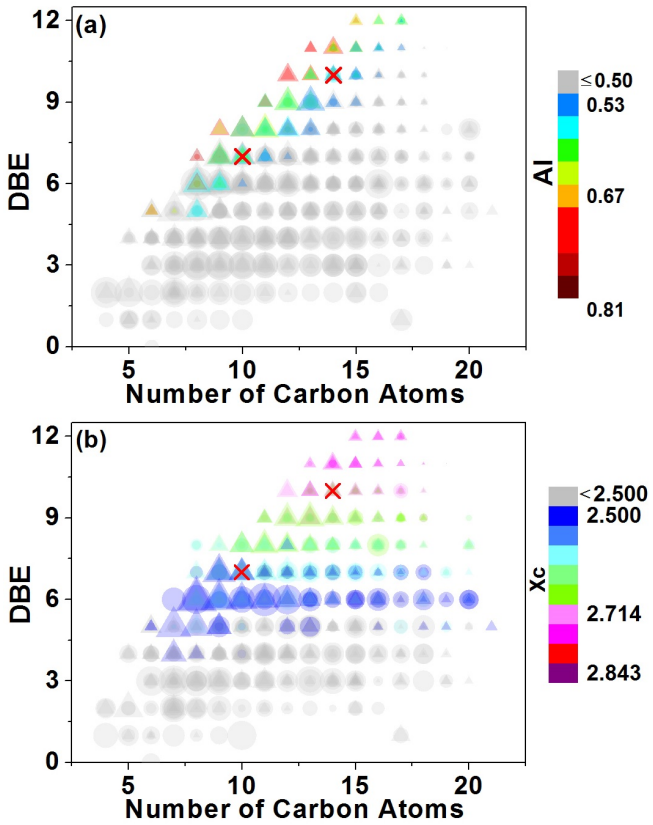


**Figure 4.** Double bond equivalents (DBEs) versus number of carbon atoms, (a) aromaticity index (AI), and (b) aromaticity equivalent ($X_c$) of all CHO formulae in the Birmingham background (circles) and tunnel (triangle) samples. The red crosses indicate a two- and three-ring PAH (naphthalene ($C_{10}H_8$) and anthracene ($C_{14}H_{10}$)). The grey points indicate non-aromatic formulae with AI≤0.50 or $X_c$<2.500. A significant number of non-aromatic formulae with DBE>6 is clearly visible in both samples. Only formulae with DBE>9 and $X_c$>2.7 can be clearly assigned as PAHs. The size of the symbols reflects the relative peak intensities in the mass spectra on a logarithmic scale.

Journal Name

ARTICLE

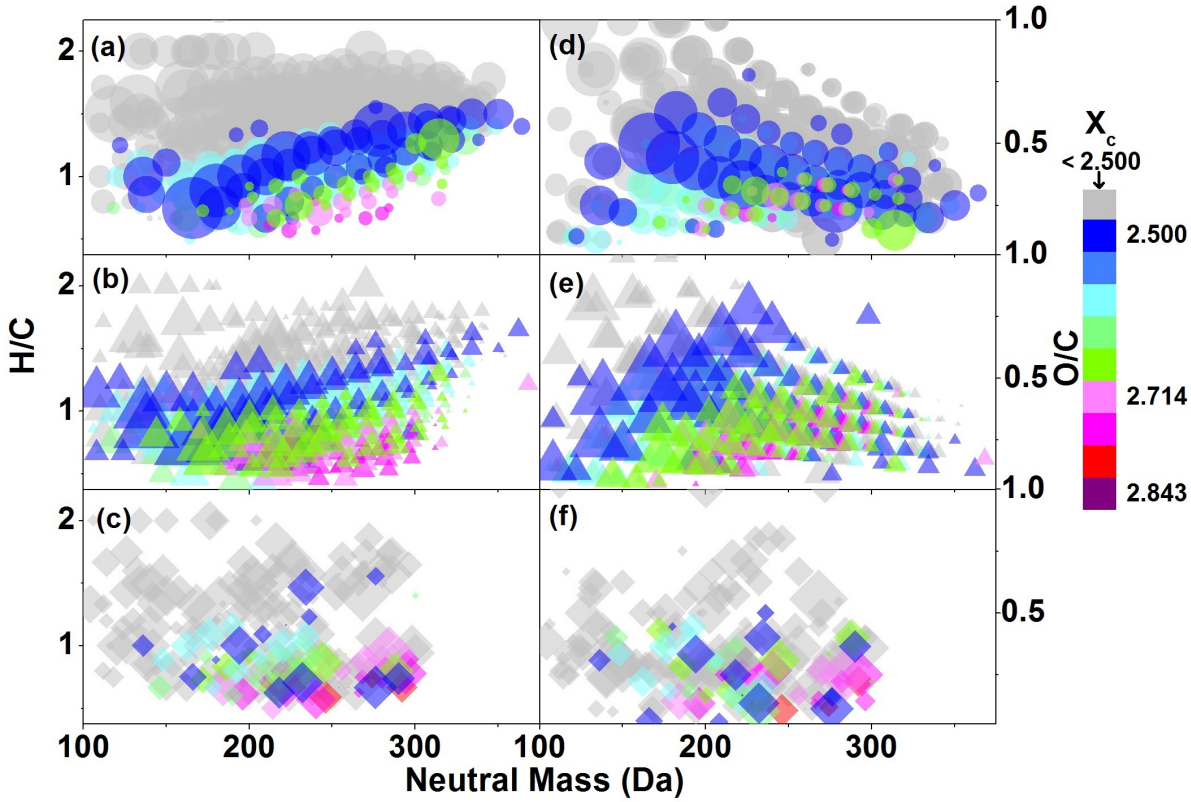


**Figure 5.** H/C (a, b and c) and O/C (d, e and f) values of all CHO formulae are shown as a function of their neutral mass from Birmingham background (a and d), tunnel (b and e) and Cork harbour (c and f) samples with their $X_c$ values color-coded. Grey data points indicate non-aromatic compounds ($X_c < 2.5$), blue to green data ($2.5 < X_c < 2.7$) are mono-aromatic compounds and pink to purple data ($X_c > 2.7$) includes PAHs. The size of the symbols reflects the relative peak intensities in the mass spectra on a logarithmic scale.

Journal Name

ARTICLE

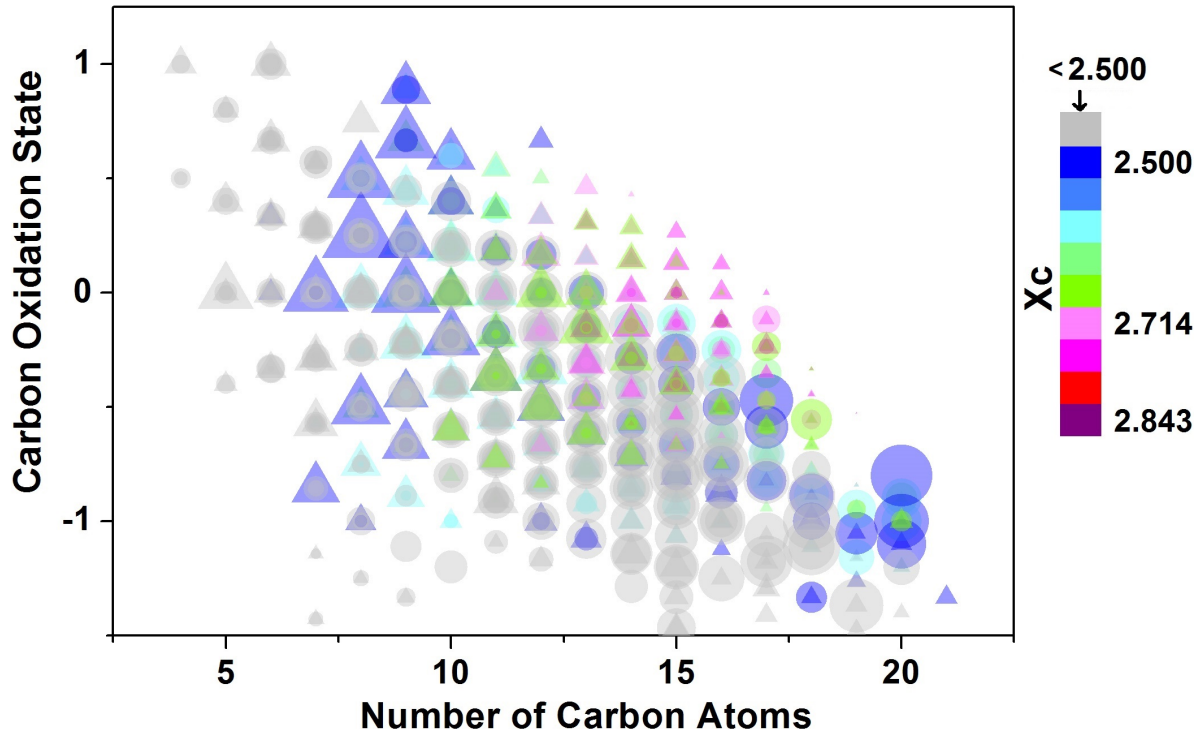


**Figure 6.** Carbon oxidation state versus the carbon atom number of all CHO formulae in the Birmingham tunnel (triangle) and Birmingham background (circles) formulae ($X_c$ values color-coded). Especially for the tunnel samples, the high degree of alkylation of moon-aromatics with up to 10-11 carbon atoms is clearly visible as well as the generally lower degree of oxidation of PAHs (i.e. lower carbon oxidation state values) compared to mono-aromatics. The size of the symbols reflects the relative peak intensities in the mass spectra on a logarithmic scale.

Journal Name

ARTICLE

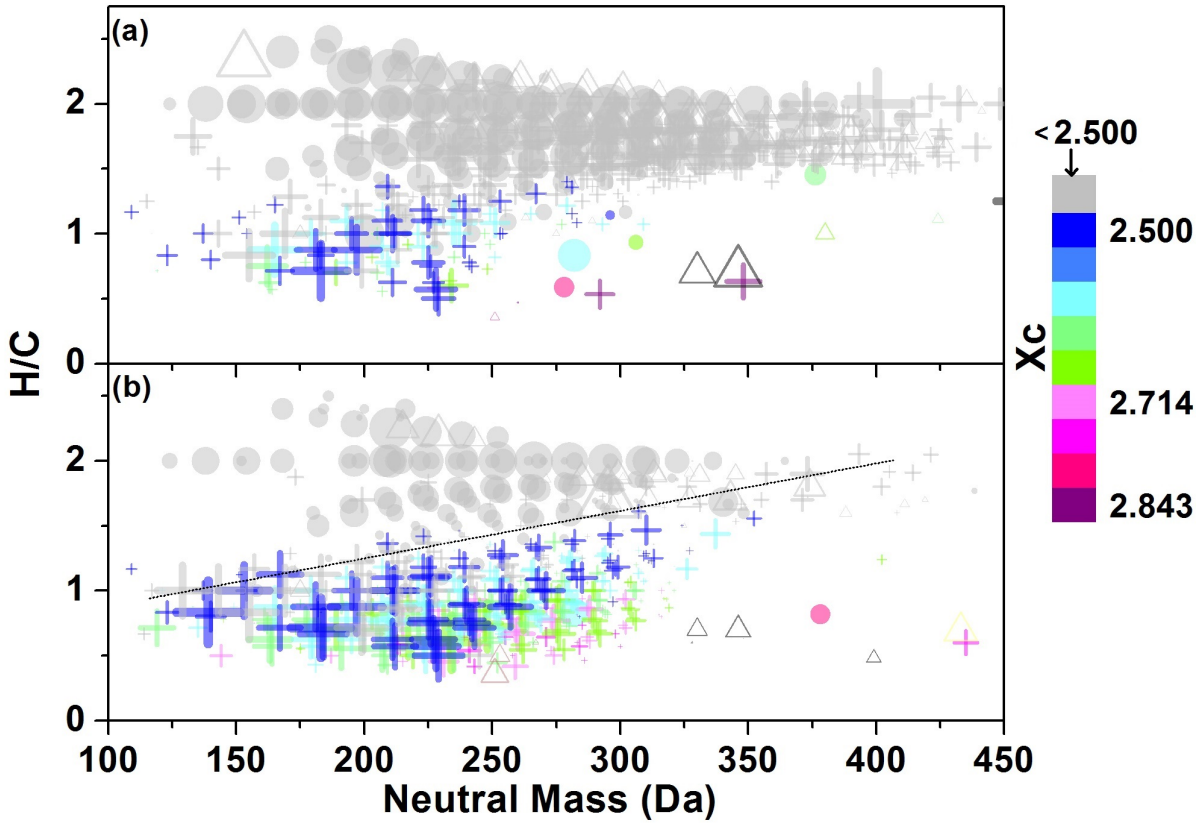


**Figure 7.** H/C atomic ratios versus molecular mass of common ions of all CHON (crosses), CHOS (circles) and CHONS (triangles) formulae in the Birmingham background (a) and tunnel (b) samples ($X_c$ values color-coded). Aerosol particles in the tunnel samples include significantly higher numbers of nitrogen-containing (poly-)aromatic formulae. The size of the symbols reflects the relative peak intensities in the mass spectra on a logarithmic scale.

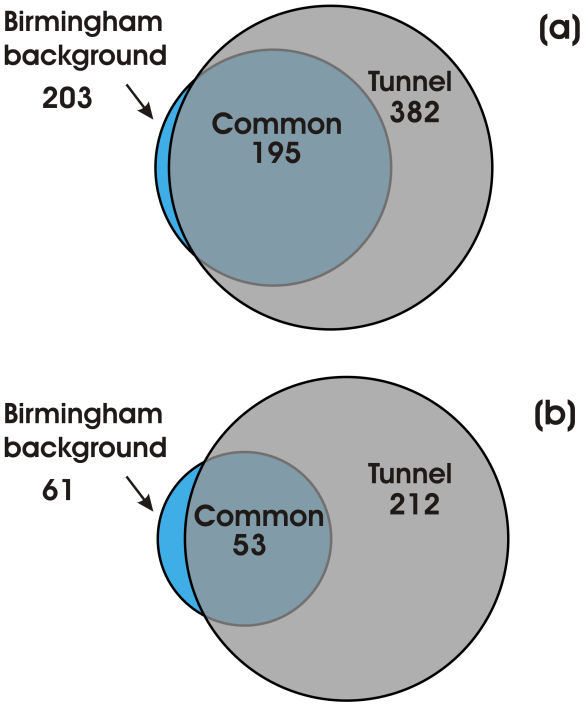


**Figure 8.** Venn diagrams showing the number of molecular formulae associated with (a) mono-aromatic and (b) PAH-like species in the Birmingham tunnel and background samples and common formulae present at both locations. The size of the circles reflects the relative ratio of molecular formulae identified in the samples.